RAA 2018 Vol. **18** No. **6**, 72(12pp) doi: 10.1088/1674–4527/18/6/72

http://www.raa-journal.org *http://iopscience.iop.org/raa*

Research in Astronomy and Astrophysics

Physical and geometrical parameters of VCBS XIII: HIP 105947

Suhail Gumaan Masda[1,2], Mashhoor Ahmed Al-Wardat[3] and Jiyaulla Khan Moula Khan Pathan[4]

[1] Physics Department, Dr. Babasaheb Ambedkar Marathwada University, Aurangabad-431001, Maharashtra, India; *suhail.masda@gmail.com*

[2] Physics Department, Hadhramout University, PO Box 50511, Mukalla, Yemen

[3] Dept. of Physics and Institute of Astronomy and Space Sciences, Al al-Bayt University, PO Box 130040, Mafraq, 25113 Jordan

[4] Physics Department, Maulana Azad College, Aurangabad-431001, Maharashtra, India

Received 2017 September 24; accepted 2018 February 8

Abstract The best physical and geometrical parameters of the main sequence close visual binary system (CVBS), HIP 105947, are presented. These parameters have been constructed conclusively using Al-Wardat's complex method for analyzing CVBSs, which is a method for constructing a synthetic spectral energy distribution (SED) for the entire binary system using individual SEDs for each component star. The model atmospheres are in its turn built using the Kurucz (`ATLAS9`) line-blanketed plane-parallel models. At the same time, the orbital parameters for the system are calculated using Tokovinin's dynamical method for constructing the best orbits of an interferometric binary system. Moreover, the mass-sum of the components, as well as the $\Delta\theta$ and $\Delta\rho$ residuals for the system, is introduced. The combination of Al-Wardat's and Tokovinin's methods yields the best estimations of the physical and geometrical parameters. The positions of the components in the system on the evolutionary tracks and isochrones are plotted and the formation and evolution of the system are discussed.

Key words: binaries: close — binaries: visual — stars: fundamental parameters — stars: individual (HIP 105947)

1 INTRODUCTION

Studies of duplicity and multiplicity of stars in the Galaxy have shown that their ratio reaches 50 per cent among nearby solar-type main sequence stars (Duquennoy & Mayor 1991), and 42 per cent among nearby M stars (Fischer & Marcy 1992). Most of these stars are either visually close enough to each other or far enough away that they appear as single stars, i.e. the separation angle between the components is small. These cases are called close visual binary stars (CVBSs).

One of the goals of the *Hipparcos* mission was to reveal the duplicity of these stars, and data from that mission were used to identify thousands of resolved stars and their relative position measurements. At the same time and later on, several astronomical groups used special techniques like speckle interferometry and adaptive optics with ground-based telescopes to observe these stars and to measure their relative positions and magnitude differences.

The study and analysis of stellar binary systems are an extremely popular topic that has yielded many results, especially related to the estimations of stellar masses and distances, which are usually derived in a reasonable way from accurate analysis of synthetic spectra, Keplerian motions, radial velocity curves and theoretical evolutionary tracks (Dryomova & Svechnikov 2003; Malkov et al. 2010).

Some of the physical and geometrical parameters can be estimated directly in the cases of eclipsing and spectroscopic binaries, but there is no direct way to estimate the parameters of CVBSs (Al-Wardat et al. 2017). So, Al-Wardat's complex method for analyzing CVBSs (Al-Wardat et al. 2016) represents an indirect method which combines measurements of magnitude difference from speckle interferometry with the system's entire spectral energy distribution (SED) from spectrophotometry along with atmospheric modeling to estimate the physical and geometrical parameters, and it was combined with Tokovinin's method for dynamical analysis (Tokovinin 1992) to get the complete set of these parameters for individual components of a binary system.

The method has been applied with substantial success to several solar-type stars like ADS 11061, COU 1289, COU 1291, HIP 11352, HIP 11253, HIP 70973, HIP 72479, Gliese 150.2, Gliese 762.1, COU 1511 and FIN 350 (Al-Wardat 2002, 2007, 2009; Al-Wardat & Widyan 2009; Al-Wardat 2012; Al-Wardat et al. 2014b, 2016; Masda et al. 2016; Al-Wardat et al. 2017), and to more rare instances like sub-giant binary systems HD 25811, HD 375 and HD 6009 (Al-Wardat et al. 2014c,a; Al-Wardat 2014).

This paper, the 13th in a series, presents the complete collection of physical and geometrical parameters for the solar-type close visual binary system HIP 105947 (HD 204236).

As a matter of fact, HIP 105947 has been identified as a solar neighborhood CVBS located at a kinematic distance of 57.21 ± 0.003 pc (17.48 ± 1.02 mas) (van Leeuwen 2007) and its measured separation is less than or equal to $0.2''$. The system was detected by the *Hipparcos* mission and the first observation was given in the 1991.25 epoch of the Hipparcos catalog (ESA 1997).

The first orbit of HIP 105947 was calculated by Balega et al. (2006) from implementing the Monet (1977) method. Their estimated mass-sum was $2.68 \pm 0.58\,M_\odot$ using the old *Hipparcos* parallax of 17.11 ± 1.13 mas (ESA 1997). Subsequently, it was modified by Mason et al. (2010) through utilizing the methods described by Hartkopf et al. (2001). Their estimated mass-sum was $2.30 \pm 1.14\,M_\odot$ using the revised *Hipparcos* parallax of 17.48 ± 1.02 mas (van Leeuwen 2007). The last observed relative position measurement applied by Mason et al. (2010) was at epoch 2009.6707. So, five new observational points from epoch 2010.4818 to epoch 2015.4974 are included in our modified orbit (Table 1).

2 OBSERVATIONAL DATA

The entire observational SED for the system HIP 105947 was taken from Al-Wardat (2003) (Fig. 1, reproduced with author's permission), and it was used as reference for comparison with the entire synthetic SED. The observational SED (Fig. 1) was obtained with a low-resolution grating ($325/4°$ grooves/mm, 5.97 Å/px reciprocal dispersion) that is part of the UAGS spectrograph at the 1 m (Zeiss-1000) telescope administered by SAO-Russia, and it covers the approximate wavelength range of $\lambda = 3700$ to 8000 Å.

Table 2 displays the fundamental data on HIP 105947. These data were taken from the SIMBAD database, NASA/IPAC, the Hipparcos and Tycho Catalogs (ESA 1997) and Strömgren photometry. Table 3 shows the magnitude difference Δm between the components of the system along with filters used in the observation expressed in nm and a reference for each value from the Fourth Catalog of Interferometric Measurements of Binary Stars (INT4)[1].

3 METHOD AND ANALYSIS

3.1 HIP 105947

The visual magnitude of the binary ($m_v(V_J)$) and magnitude difference between its components (Δm) are the requirements for applying Al-Wardat's complex method to analyze CVBSs. Together, they lead to determination of the apparent magnitudes for individual components of the system using the following simple relationships:

$$m_v^A = m_v + 2.5\log(1 + 10^{-0.4\Delta m}), \quad (1)$$

$$m_v^B = m_v^A + \Delta m, \quad (2)$$

and their errors are expressed with the following equations:

$$\sigma^2_{m_v^A} = \sigma^2_{m_v} + \left(\frac{1}{1 + 10^{+0.4\Delta m}}\right)^2 \sigma^2_{\Delta m}, \quad (3)$$

$$\sigma^2_{m_v^B} = \sigma^2_{m_v^A} + \sigma^2_{\Delta m}\,. \quad (4)$$

For the system HIP 105947, the mean speckle-interferometric magnitude difference was taken as 1.53 ± 0.07 mag, which is the average of all Δm measurements under different speckle filters for V-band filters (534–562) nm with different bandwidths (see Table 3), which represent the closest filters to V_J.

This value was implemented concurrently with the entire visual magnitude of the system, $m_v = 7.53$ mag, (Table 2) in Equations (1) and (2), and resulted in calculating the individual apparent magnitudes of the components of the system as $m_v^A = 7.77 \pm 0.01$ mag and

[1] *http://www.usno.navy.mil/USNO/astrometry/optical-IR-prod/wds/int4*

Table 1 New Data from Interferometric Measurements of the HIP 105947 System

	Data Epoch	θ ($^\circ$)	ρ ($''$)	$(\lambda/\Delta\lambda)$ (nm)	Telescope* (m)	Reference
HIP 105947	2010.4818	165.5	0.1788	562/40	3.5	Horch et al. (2011)
	2013.7363	225.8	0.0850	534 /22	4.1	Tokovinin et al. (2014)
	2014.7629	266.6	0.0726	778/132	4.2	Tokovinin et al. (2015)
	2015.4974	304.4	0.0908	543/22	4.1	Tokovinin et al. (2016)
	2015.4974	304.8	0.0952	788/132	4.1	Tokovinin et al. (2016)

Notes: * Telescope aperture in meters where the observations were obtained.

Table 2 Observational data from the SIMBAD database and magnitudes and color indices from the Hipparcos and Tycho Catalogs and Strömgren photometry for the HIP 105947 system.

Property	HIP 105947 HD 204236	Source of data
α_{2000} [1]	$21^{\rm h}27^{\rm m}23.255^{\rm s}$	SIMBAD[2]
δ_{2000} [3]	$-07^\circ00'56.95''$	–
SAO	145409	–
Sp. Typ.	F8	–
$E(B-V)$	0.10 ± 0.003	NASA/IPAC[4]
A_V	0.31 ± 0.003	–
V_J(Hip)	7.53	ESA (1997)
B_J	8.10 ± 0.02	Høg et al. (2000)
$(V-I)_J$	0.67 ± 0.01	ESA (1997)
$(B-V)_J$	0.60 ± 0.02	–
$B_{\rm T}$	8.24 ± 0.02	Høg et al. (2000)
$V_{\rm T}$	7.59 ± 0.01	Høg et al. (2000)
$(u-v)_S$	0.95 ± 0.02	Hauck & Mermilliod (1998)
$(v-b)_S$	0.56 ± 0.01	Hauck & Mermilliod (1998)
$(b-y)_S$	0.37 ± 0.00	Hauck & Mermilliod (1998)
$\pi_{\rm Hip}$ (mas)	17.11 ± 1.13	ESA (1997)
$\pi_{\rm Hip}$ (mas)	17.48 ± 1.02	van Leeuwen (2007)

Notes: [1] Right Ascension; [2] *http://simbad.u-strasbg.fr/simbad/sim-fid;* [3] Declination; [4] Schlegel et al. (1998).

$m_v^B = 9.30 \pm 0.07$ mag for the primary and secondary components of the system, respectively.

Using the updated *Hipparcos* parallax of $\rm d = 57.21 \pm 0.003$ pc (van Leeuwen 2007), with the following relation

$$M_V - m_v = 5 - 5\log(\rm d) - A_V, \tag{5}$$

the absolute magnitudes along with their errors are: $M_V^A = 3.98 \pm 0.13$ mag and $M_V^B = 5.51 \pm 0.14$ mag. Note that the interstellar extinction can be neglected ($A_V \approx 0$) because the system is nearby.

Errors in the absolute magnitudes were calculated using the following relation

$$\sigma^2_{M_V^*} = \sigma^2_{m_v^*} + \left(\frac{\log \rm e}{0.2\pi_{\rm Hip}}\right)^2 \sigma^2_{\pi_{\rm Hip}}\,; \quad * = A, B\,. \tag{6}$$

where $\sigma_{m_v^*}$ are errors in the apparent magnitudes of the A and B components given in Equations (3) and (4).

Hence, depending on the estimated preliminary absolute magnitudes, the preliminary values of the effective temperature and gravitational acceleration for each component were referenced from tables in Lang (1992) and Gray (2005) as follows: $T_{\rm eff} = 6200$ K, $\log g = 4.31$ for the primary component and $T_{\rm eff} = 5490$ K, $\log g = 4.47$ for the secondary component.

Note that for solar-type stars, these parameters are related to other parameters according to the following equations:

$$\log \frac{R}{R_\odot} = \frac{M_{\rm bol}^\odot - M_{\rm bol}}{5} - 2\log\frac{T_{\rm eff}}{T_\odot}, \tag{7}$$

$$\log g = \log \frac{M}{M_\odot} - 2\log\frac{R}{R_\odot} + \log g_\odot, \tag{8}$$

Table 3 Magnitude difference between the components of the HIP 105947 system and available errors, along with filters used to obtain the observations.

Δm (mag)	$\sigma_{\Delta m}$	Filter ($\lambda/\Delta\lambda$) (nm)	Reference
1.17	0.60	$V_{\rm Hip}$: 550/40	[1]
1.50	0.04	545/30	[2]
1.40	0.02	545/30	[3]
1.29	0.05	850/75	[3]
1.31	0.06	600/30	[3]
1.47	0.03	545/30	[4]
1.56	*	550/40	[5]
1.56	*	550/40	[6]
2.00	*	551/22	[7]
1.40	*	657/05	[7]
1.50	*	551/22	[7]
1.50	*	788/132	[8]
1.37	*	692/40	[9]
1.44	*	562/40	[9]
1.90	*	534/22	[10]
1.10	*	788/132	[11]
1.30	*	543/22	[12]
1.50	*	788/132	[12]

Notes: * The errors are not given in INT4. Reference: [1] ESA (1997); [2] Pluzhnik (2005); [3] Balega et al. (2006); [4] Balega et al. (2007); [5] Horch et al. (2008); [6] Horch et al. (2010); [7] Tokovinin et al. (2010b); [8] Tokovinin et al. (2010a); [9] Horch et al. (2011); [10] Tokovinin et al. (2014); [11] Tokovinin et al. (2015); [12] Tokovinin et al. (2016).

where $T_\odot = 5777\,\mathrm{K}$, $M_{\rm bol}^{\odot} = 4.75\,\mathrm{mag}$ and $\log g_\odot = 4.44$. $M_{\rm bol} = M_V$+BC; BC indicates the bolometric correction.

Now, we have the preliminary input parameters to build model atmospheres for each individual component of the system, and to do so we use `ATLAS9` line-blanketed model atmospheres of Kurucz (1994).

In order to construct a synthetic SED of a star from its model atmosphere, we need information about its distance d and radius R. The first parameter d was taken from the updated *Hipparcos* parallax ($d = 57.21 \pm 0.003\,\mathrm{pc}$) as a postulated value with its error, while the second parameter is subject to change within the values of the observational data like the entire SED, magnitudes and color indices.

The method makes use of the entire observational SED as a reference guide for the best-fitted entire synthetic SED, in an iterative way. The entire synthetic SED of the binary system, which is connected to the energy flux of the individual components A and B located at a distance d (pc) from the Earth, is calculated using the following equation

$$F_\lambda \cdot d^2 = H_\lambda^A \cdot R_A^2 + H_\lambda^B \cdot R_B^2. \tag{9}$$

This equation can be written as

$$F_\lambda = \left(\frac{R_A}{d}\right)^2 \left(H_\lambda^A + H_\lambda^B \left(\frac{R_B}{R_A}\right)^2\right), \tag{10}$$

where F_λ is the flux for the entire synthetic SED of the binary system at the Earth, H_λ^A and H_λ^B are the fluxes of the primary and secondary star respectively, in units of $\mathrm{erg\,cm^{-2}\ s^{-1}\ Å^{-1}}$, while R_A and R_B are the radii of the primary and secondary components respectively of the binary system in solar units.

Many attempts were carried out find the best-fit between the synthetic and observational SEDs. Hence, the physical and geometrical parameters of the best-fitted synthetic SED adequately represent the parameters of the system's components within error limits of the observational SED.

It is very important to mention here that values of the radii are totally reliant on the precision of *Hipparcos* parallax measurements (see Eq. (10)), which in some cases are distorted by the orbital motion of the components of such systems as pointed out by Shatskii & Tokovinin (1998).

The parameters which led to the best-fit are as follows (Fig. 1):

$$T_{\rm eff}^A = 6230 \pm 80\,{\rm K}, T_{\rm eff}^B = 5470 \pm 80\,{\rm K},$$

$$\log g_A = 4.30 \pm 0.07, \log g_B = 4.45 \pm 0.08\,,$$

$$R_A = 1.443 \pm 0.06\,R_\odot, R_B = 0.989 \pm 0.05\,R_\odot\,.$$

Errors in the radii were estimated from the method and double-checked using the following equation

$$\sigma_R \approx \pm R \sqrt{\left(\frac{\sigma_{M_{\rm bol}}}{5\log e}\right)^2 + 4\left(\frac{\sigma_{T_{\rm eff}}}{T_{\rm eff}}\right)^2}\,. \tag{11}$$

The individual stellar luminosities and bolometric magnitudes of the system are $L_A = 2.816 \pm 0.30\,L_\odot$, $L_B = 0.786 \pm 0.10\,L_\odot$ and $M_{\rm bol}^A = 3.63 \pm 0.08$ mag, $M_{\rm bol}^B = 5.01 \pm 0.09$ mag, respectively.

Based on the final effective temperatures and stellar luminosities of the binary system, we put the components of the binary system on the theoretical Hertzsprung-Russell (H-R) diagram. The positions of the components of the system on the H-R diagram lead to theoretical estimates of the masses and ages of the binary system and the spectral types of the components of the system were estimated as follows: F8 and G7.5 for the primary and secondary components of the system, respectively. Using this analysis, the masses of the components can be estimated as: $M^A = 1.21 \pm 0.21\,M_\odot$ and $M^B = 0.89 \pm 0.15\,M_\odot$ with spectral types F8 for the primary and G7.5 for the secondary. The age of the system is $t_{\rm T} \approx 2.75 \pm 0.06$ Gyr.

4 SYNTHETIC PHOTOMETRY

Notwithstanding the significance and simplicity of the direct comparison between synthetic and observed spectra in determining the best-fit, there is another powerful and quantitative technique that examines this fitting, which is synthetic photometry. It helps us to calculate the apparent magnitudes and color indices of the entire and individual SEDs in any photometrical system, and enables us to compare the synthetic photometry with observational one.

The apparent magnitude for a specific photometric filter can be computed using the following equation: (Maíz Apellániz 2007; Al-Wardat 2012)

$$m_p[F_{\lambda,s}(\lambda)] = -2.5 \log \frac{\int P_p(\lambda) F_{\lambda,s}(\lambda) \lambda {\rm d}\lambda}{\int P_p(\lambda) F_{\lambda,r}(\lambda) \lambda {\rm d}\lambda} + {\rm ZP}_p\,, \tag{12}$$

where m_p is the synthetic magnitude of the passband p, $P_p(\lambda)$ is the dimensionless sensitivity function of the passband p, $F_{\lambda,s}(\lambda)$ is the synthetic SED of the object and $F_{\lambda,r}(\lambda)$ is the SED of the reference star (Vega). Zero points (ZP$_p$) from Maíz Apellániz (2007) are adopted.

The calculated magnitudes and color indices of the individual components and entire synthetic SEDs for the system, in different photometrical systems (Johnson-Cousins: $U, B, V, R, U-B, B-V, V-R$; Strömgren: $u, v, b, y, u-v, v-b, b-y$ and Tycho: $B_{\rm T}, V_{\rm T}, B_{\rm T}-V_{\rm T}$), are listed in Table 4.

Table 6 shows the final physical and geometrical parameters of the individual components for the system. Figure 1 shows the best fit between the entire synthetic and observational SED along with the SED for each individual component presented for the first time.

5 ORBITS AND MASSES

5.1 Orbits

The orbital solution also plays a vital role in calculating stellar masses. This solution involves the orbital period P (in years); the eccentricity e; the semi-major axis a (in arcsec); the inclination i (in degrees); the argument of periastron ω (in degrees); the position angle of nodes Ω (in degrees); and the time of primary minimum T_0 (in years).

In order to derive the orbital parameters for the system, we followed Tokovinin's dynamical method (Tokovinin 1992). The method performs a least-squares adjustment to all available relative position measurements and radial velocities (once available), with weights inversely proportional to the square of their standard errors.

The initial determinations of the orbital parameters were carried out based on four parameters (P, T, e and a). These parameters are intrinsically important for applying the least-squares method and then deriving the other orbital parameters.

The results of the dynamical analysis and orbital solutions of HIP 105947 are listed in Table 7, and the orbit is shown in Figure 2.

5.2 Masses

As formerly mentioned, the mass is an intrinsically crucial parameter because the mass of a star determines its present and future, i.e. the birth, life and death of a star. As a result, using the estimated orbital solutions for the

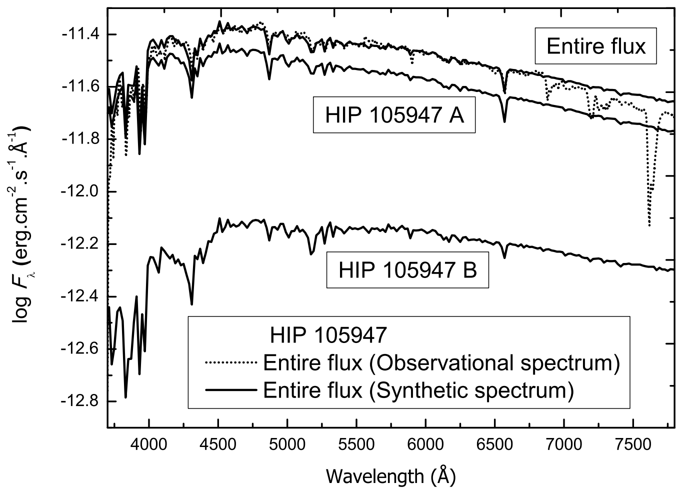

Fig. 1 The entire synthetic SED of the system HIP 105947 (built using parameters given in Table 6 like $T_{\rm eff}$, $\log g$, R and parallax) versus the observational one. The figure also shows the synthetic SED for each component.

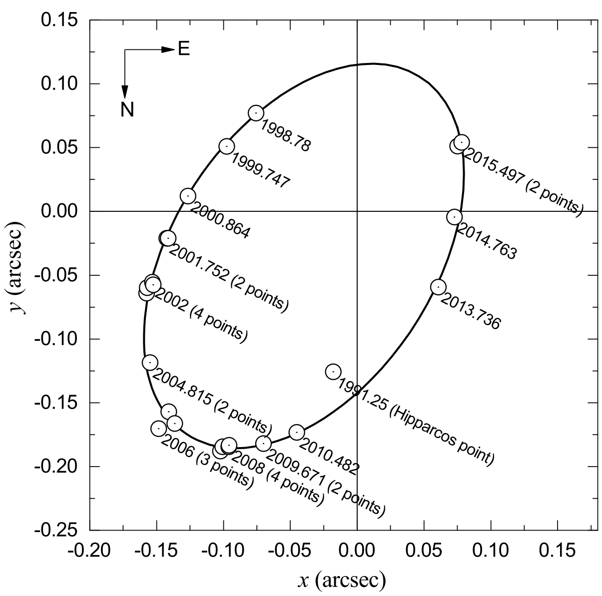

Fig. 2 The relative orbit of the binary system HIP 105947 constructed using the relative position measurements from INT4. The origin point represents the position of the primary component.

system in Table 7, period and semi-major axis, combined with the revised *Hipparcos* parallax (van Leeuwen 2007) for the system, let us calculate the total mass along with its error for the system according to Kepler's third law

$$M_{\rm Tot.} = M_A + M_B = \left(\frac{a^3}{\pi^3 P^2}\right) M_\odot \,, \qquad (13)$$

$$\frac{\sigma_M}{M} = \sqrt{9\left(\frac{\sigma_\pi}{\pi}\right)^2 + 9\left(\frac{\sigma_a}{a}\right)^2 + 4\left(\frac{\sigma_P}{P}\right)^2}\,, \qquad (14)$$

where P is the orbital period (in years), M_A and M_B are the masses (in solar mass), and a and π are the semi-major axis and the *Hipparcos* parallax (both in arcsec), respectively. Using Equation (13), we obtained the mass-sum for HIP 105947 as $2.06 \pm 0.36\,M_\odot$.

Comparing this result with the estimated masses using Al-Wardat's method by plotting the positions of the components on the H-R diagram (see Table 6 and Fig. 3), we find a good coincidence between them. This means that the analysis in both methods as well as the combination of two methods together was successful, and consequently obtained the precise physical and geometrical parameters of the studied CVBS.

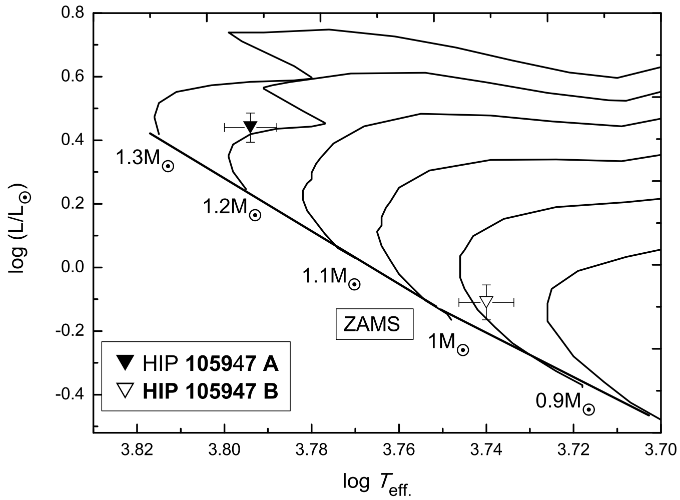

Fig. 3 The evolutionary tracks of both components of HIP 105947 on the H-R diagram with masses (0.8, 0.9, ..., 1.3 $M_{\odot}$). The evolutionary tracks were taken from Girardi et al. (2000b).

Table 4 Magnitudes and Color Indices of the Entire Synthetic Spectrum and Individual Components of HIP 105947

Sys.	Filter	Entire Synth. $\sigma = \pm 0.03$	HIP 105947 A	HIP 105947 B
Johnson-Cousins	U	8.24	8.39	10.47
	B	8.13	8.32	10.10
	V	7.53	7.77	9.30
	R	7.20	7.46	8.88
	$U-B$	0.11	0.07	0.37
	$B-V$	0.60	0.55	0.79
	$V-R$	0.33	0.30	0.42
Ström.	u	9.40	9.56	11.61
	v	8.45	8.63	10.52
	b	7.87	8.08	9.73
	y	7.50	7.74	9.27
	$u-v$	0.95	0.93	1.09
	$v-b$	0.59	0.55	0.79
	$b-y$	0.37	0.34	0.47
Tycho	$B_{\rm T}$	8.27	8.45	10.31
	$V_{\rm T}$	7.60	7.83	9.39
	$B_{\rm T}-V_{\rm T}$	0.67	0.62	0.92

6 RESULTS AND DISCUSSION

The results of combining Al-Wardat's complex method for analyzing CVBSs with Tokovinin's dynamical method in analyzing the CVBS, HIP 105947, are presented.

Table 5 lists the residuals, $\Delta\theta$ and $\Delta\rho$, and root mean square (rms) for HIP 105947. The results of the orbital solutions exhibit slight modifications in the orbital parameters. The rms values for our orbital solutions are 0.60° and $0.0015''$ for HIP 105947.

Table 7 summarizes the ultimate results of our orbital solutions with former studies for the system, and the orbit is plotted in Figure 2.

Table 8 displays a very good agreement between the synthetic magnitudes and color indices with the observational ones for the system. This reflects the best-fit between the synthetic and observational SED and hence the reliability of Al-Wardat's complex method in estimating the physical and geometrical parameters of CVBS. Without a doubt, this gives a lucid and powerful indica-

Table 5 Relative Position Measurements

Epoch	θ ($^\circ$)	ρ ($''$)	Ref.	$\Delta\theta$ ($^\circ$)	$\Delta\rho$ ($''$)
1991.25	171.64	0.1266	[1]	–11.1	–0.008
1997.7201	177.6 *	0.151	[2]	–	–
1998.7796	219.2**	0.108	[3]	5.7	–0.001
1999.7468	242.2**	0.110	[3]	0.3	–0.002
2000.8643	84.6	0.127	[4]	0.1	–0.000
2001.7523	98.5	0.144	[4]	0.3	–0.000
2001.7523	98.5	0.143	[4]	0.3	–0.001
2002.7986	112.2	0.170	[5]	1.6	0.005
2002.7987	110.9	0.168	[5]	0.3	0.003
2002.799	110.0	0.163	[2]	–0.6	–0.002
2002.799	110.7	0.163	[2]	0.1	–0.002
2004.815	127.5	0.195	[2]	–0.2	–0.004
2004.8152	127.5	0.195	[6]	–0.3	–0.004
2006.4436	138.2	0.211	[5]	–0.2	–0.003
2006.5254	139.0	0.226	[7]	0.1	0.011
2006.6870	140.7	0.215	[5]	0.8	–0.000
2008.4613	151.5	0.214	[8]	0.7	0.003
2008.5430	151.5	0.2102	[9]	0.2	–0.001
2008.7669	152.6	0.2084	[9]	–0.1	–0.000
2008.7669	152.5	0.2073	[9]	–0.2	–0.001
2009.6706	159.0	0.1951	[10]	0.0	–0.001
2009.6707	159.0	0.195	[11]	0.0	–0.001
2010.4818 ***	165.5	0.1788	[12]	0.1	–0.001
2013.7363 ***	225.8	0.0850	[13]	–2.5	0.003
2014.7629 ***	266.6	0.0726	[14]	–10.1	–0.006
2015.4974 ***	304.4	0.0908	[15]	–0.4	–0.004
2015.4974 ***	304.8	0.0952	[15]	0.0	0.001
rms				0.60	0.0015

Notes: Residuals $\Delta\theta$ and $\Delta\rho$ (our work) and rms for HIP 105947, which are used to construct the orbit of the system; θ and ρ are taken from INT4; * It was neglected in our orbits (Mason et al. 1999); ** These points were modified by 180° to achieve consistency with nearby points; *** New observations in our orbit. [1] ESA (1997); [2] Balega et al. (2006); [3] Balega et al. (2002a); [4] Balega et al. (2002b); [5] Balega et al. (2013); [6] Balega et al. (2007); [7] Horch et al. (2008); [8] Horch et al. (2010); [9] Tokovinin et al. (2010b); [10] Tokovinin et al. (2010a); [11] Mason et al. (2010); [12] Horch et al. (2011); [13] Tokovinin et al. (2014); [14] Tokovinin et al. (2015); [15] Tokovinin et al. (2016).

tion for the reliability of the estimated physical and geometrical parameters of the individual components for the system as shown in Table 6.

The stellar masses for the system were calculated using two independent methods: Al-Warda's complex method for analyzing CVBSs and Tokovinin's dynamical method for orbital solutions of binary stars. The former gives $2.10 \pm 0.19\,M_\odot$ for HIP 105947 (see Fig. 3 and Table 6), while the latter yields $2.06 \pm 0.36\,M_\odot$ for HIP 105947 (see Table 7). Both methods used the revised *Hipparcos* parallax (van Leeuwen 2007).

A fast look and comparison with old orbital parameters for the system indicate that for HIP 105947, Balega et al. (2006) used the old *Hipparcos* parallax (ESA 1997) to estimate the masses, whereas Mason et al. (2010) used the revised *Hipparcos* parallax but their eccentricity e and semi-major axis a were to a certain extent high, unlike Balega et al. (2006) and ours. Of course, these discrepancies are due to the availability of new observational measurements provided by INT4.

Table 4 lists the results of the synthetic photometry for the entire system and individual components of HIP 105947, in different photometrical systems (Johnson-

Table 6 The Estimated Parameters of the Individual Components of HIP 105947

Parameters	Units	HIP 105947	
		HIP 105947 A	HIP 105947 B
$T_{\text{eff}} \pm \sigma_{T_{\text{eff}}}$	[K]	6230 ± 80	5470 ± 80
$R \pm \sigma_R$	$[R_\odot]$	1.443 ± 0.06	0.989 ± 0.05
$\log g \pm \sigma_{\log g}$	[cgs]	4.30 ± 0.07	4.45 ± 0.08
$L \pm \sigma_L$	$[L_\odot]$	2.816 ± 0.30	0.786 ± 0.10
$M_{\text{bol}} \pm \sigma_{M_{\text{bol}}}$	[mag]	3.63 ± 0.08	5.01 ± 0.09
$M_V \pm \sigma_{M_V}$	[mag]	3.98 ± 0.13	5.51 ± 0.14
$M^a \pm \sigma_M$	$[M_\odot]$	1.21 ± 0.21	0.89 ± 0.15
Sp. Type^b		F8	G7.5
Parallax ^{c}	[mas]	17.48 ± 1.02	
$(M_A + M_B)^d$	$[M_\odot]$	2.06 ± 0.36	
Age ^{e}	[Gyr]	2.75 ± 0.06	

Notes: ^{a} Depending on the evolutionary tracks of masses (0.8, 0.9, ..., 1.3 $M_\odot$) from Girardi et al. (2000b) (Fig. 3); ^{b} By using the tables of Lang (1992); Gray (2005) and applying the $M_V - S_P$ relation; ^{c} The revised *Hipparcos* parallax of 57.21 ± 0.003 pc for HIP 105947 (van Leeuwen 2007); ^{d} Depending on the orbital solutions and Tokovinin's method (Tokovinin 1992); ^{e} Depending on the the isochrones for low- and intermediate-mass stars with different metallicities from Girardi et al. (2000a) (Figs. 4 and 5).

Table 7 Orbital Parameter Solutions and Total Masses Formerly Published for the HIP 105947 System, for Comparison with This Work

Parameter	Units	System HIP 105947		
		(Balega et al. 2006)	(Mason et al. 2010)	This work
$P \pm \sigma_P$	[yr]	18.79 ± 0.57	20.3 ± 4.9	20.78 ± 0.06
$T_0 \pm \sigma_{T_0}$	[yr]	1993.96 ± 0.40	1994.7 ± 2.6	1994.94 ± 0.06
$e \pm \sigma_e$	-	0.354 ± 0.010	0.37 ± 0.25	0.347 ± 0.001
$a \pm \sigma_a$	[arcsec]	0.168 ± 0.003	0.171 ± 0.018	0.168 ± 0.0004
$i \pm \sigma_i$	[deg]	57.1 ± 2.1	54.5 ± 3.9	51.78 ± 0.27
$\omega \pm \sigma_\omega$	[deg]	149.1 ± 1.5	140.0 ± 14.0	148.00 ± 0.72
$\Omega \pm \sigma_\Omega$	[deg]	129.7 ± 6.4	154.0 ± 12.0	152.41 ± 0.30
$M_{\text{T}} \pm \sigma_M$	$[M_\odot]$	2.68 ± 0.58	2.30 ± 2.2	2.06 ± 0.36
$\pi_{\text{Hip}} \pm \sigma_{\pi_{\text{Hip}}}$	[mas]	$17.11 \pm 1.13\ ^a$	$17.48 \pm 1.02\ ^b$	$17.48 \pm 1.02\ ^b$

Notes: ^{a} The old *Hipparcos* parallax (ESA 1997). ^{b} The revised *Hipparcos* parallax (van Leeuwen 2007).

Table 8 Comparison between the Observational and Synthetic Magnitudes and Color Indices of the System

Filter	HIP 105947	
	Observed ^{a} (mag)	Synthetic ^{b} (This work) (mag)
V_J	7.53	7.53 ± 0.03
B_J	8.10 ± 0.02	8.13 ± 0.03
B_{T}	8.24 ± 0.02	8.27 ± 0.03
V_{T}	7.59 ± 0.01	7.60 ± 0.03
$(B-V)_J$	0.60 ± 0.02	0.60 ± 0.03
$(u-v)_S$	0.95 ± 0.015	0.95 ± 0.03
$(v-b)_S$	0.56 ± 0.003	0.59 ± 0.03
$(b-y)_S$	0.37 ± 0.000	0.37 ± 0.03
Δm	$1.53^c \pm 0.07$	$1.53^d \pm 0.05$

Notes: ^{a} Real observations (see Table 2); ^{b} Synthetic work of the HIP 105947 system by using Interactive Data Language (IDL) program (see Table 4); ^{c} The average of all Δm measurements with the speckle filter V-band in the range 534–562 nm (see Table 3); ^{d} The magnitude difference between components A and B ($\Delta m = V_J^B - V_J^A$) (see Table 4).

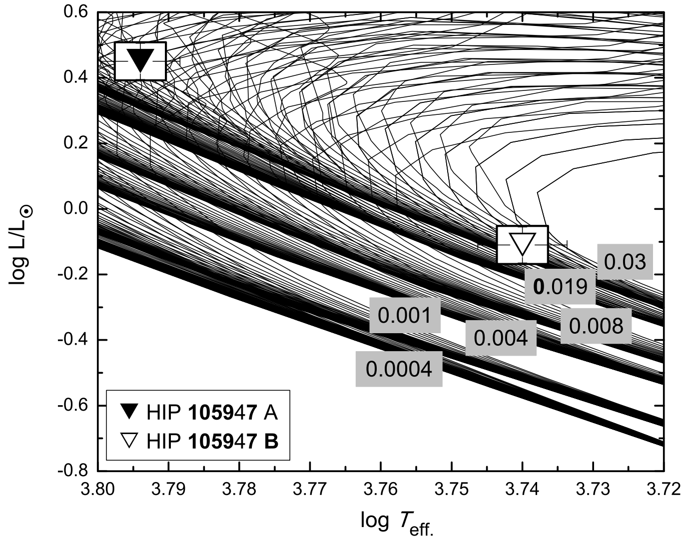

Fig. 4 The isochrones for both components of HIP 105947 on the H-R diagram for low- and intermediate-mass stars with different metallicities. The isochrones were taken from Girardi et al. (2000a).

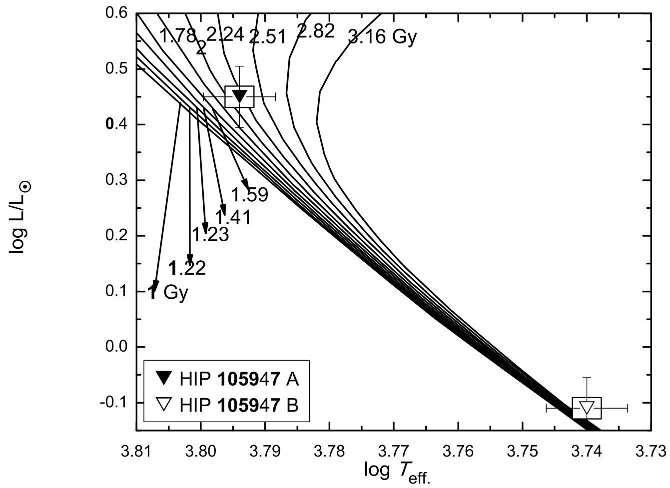

Fig. 5 The isochrones for both components of HIP 105947 on the H-R diagram for low- and intermediate-mass stars: from 0.15 to 7 $M_\odot$, and for compositions [$Z = 0.019, Y = 0.273$] of stars with different metallicities. The isochrones were taken from Girardi et al. (2000a).

Cousins: $U, B, V, R, U-B, B-V, V-R$; Strömgren: $u, v, b, y, u-v, v-b, b-y$ and Tycho: $B_{\rm T}, V_{\rm T}, B_{\rm T}-V_{\rm T}$).

The positions of the individual components of the system are shown on the evolutionary tracks of Girardi et al. (2000b) (Fig. 3). This figure indicates that both components are main sequence stars but the primary and secondary components of the system HIP 105947 are very similar to the primary and secondary components of the double-lined spectroscopic binary system HD 22128 (Folsom et al. 2013), which are well-known cases of zero-age main sequence stars. Therefore, this led us to a broad suggestion that both components of the system HIP 105947 are zero-age main sequence stars. The analysis of the system HIP 105947 shows that both of its components have an age around 2.75 ± 0.06 Gyr and solar composition [$Z = 0.019, Y = 0.273$] (Girardi et al. 2000a) (see Figs. 4 and 5).

7 CONCLUSIONS

Using Al-Wardat's method for analyzing CVBSs which employs Kurucz `ATLAS9` line-blanketed plane-parallel model atmospheres in constructing the entire and individual synthetic SEDs for a binary system, along with Tokovinin's dynamical method for orbital solutions of binary stars, we were able to estimate the complete set of physical and geometrical parameters of the main sequence CVBS HIP 105947.

The calculated entire and individual synthetic magnitudes and color indices of the system for different photometrical systems such as Johnson-Cousins $UVBR$, Strömgren $uvby$ and Tycho BV are introduced. Revised orbits and orbital parameters for the system are introduced and compared with previous studies.

The ideal positions of the components of the system are shown in a broad way on the evolutionary tracks and isochrones. The spectral types of the components of HIP 105947 are cataloged as F8 and G7.5 for the primary and secondary components of the system, respectively, with an age of 2.75 ± 0.06 Gyr.

Depending on the estimated physical and geometrical parameters of this system, the fragmentation process for the formation of such a system is the most likely scenario, where the rotating disc around an incipient central protostar in case of continuing infall and the hierarchical fragmentation during rotational collapse are the main mechanisms in producing binaries and multiple systems, as pointed out by Bonnell (1994) and Zinnecker & Mathieu (2001).

Acknowledgements This research has made use of SAO/NASA, the SIMBAD database, the Fourth Catalog of Interferometric Measurements of Binary Stars, IPAC data systems, ORBIT code and CHORIZOS code of photometric and spectrophotometric data analysis. Suhail Masda would like to thank the Human Development Fund for the scholarship and Hadhramout University in Yemen for ongoing support.

References

Al-Wardat, M. 2012, PASA, 29, 523
Al-Wardat, M. A. 2002, Bulletin of the Special Astrophysics Observatory, 53, 51
Al-Wardat, M. A. 2003, Bulletin of the Special Astrophysics Observatory, 55, 18
Al-Wardat, M. A. 2007, Astronomische Nachrichten, 328, 63
Al-Wardat, M. A. 2009, Astronomische Nachrichten, 330, 385
Al-Wardat, M. A. 2014, Astrophysical Bulletin, 69, 454
Al-Wardat, M. A., Balega, Y. Y., Leushin, V. V., et al. 2014a, Astrophysical Bulletin, 69, 58
Al-Wardat, M. A., Balega, Y. Y., Leushin, V. V., et al. 2014b, Astrophysical Bulletin, 69, 198
Al-Wardat, M. A., Docobo, J. A., Abushattal, A. A., & Campo, P. P. 2017, Astrophysical Bulletin, 72, 24
Al-Wardat, M. A., El-Mahameed, M. H., Yusuf, N. A., Khasawneh, A. M., & Masda, S. G. 2016, RAA (Research in Astronomy and Astrophysics), 16, 166
Al-Wardat, M. A., & Widyan, H. 2009, Astrophysical Bulletin, 64, 365
Al-Wardat, M. A., Widyan, H. S., & Al-thyabat, A. 2014c, PASA, 31, e005
Balega, I. I., Balega, Y. Y., Gasanova, L. T., et al. 2013, Astrophysical Bulletin, 68, 53
Balega, I. I., Balega, Y. Y., Hofmann, K.-H., et al. 2002a, A&A, 385, 87
Balega, I. I., Balega, Y. Y., Hofmann, K.-H., et al. 2006, A&A, 448, 703
Balega, I. I., Balega, Y. Y., Maksimov, A. F., et al. 2007, Astrophysical Bulletin, 62, 339
Balega, Y. Y., Tokovinin, A. A., Pluzhnik, E. A., & Weigelt, G. 2002b, Astronomy Letters, 28, 773
Bonnell, I. A. 1994, MNRAS, 269
Dryomova, G. N., & Svechnikov, M. A. 2003, Ap&SS, 283, 309
Duquennoy, A., & Mayor, M. 1991, A&A, 248, 485
ESA, ed. 1997, ESA Special Publication, 1200, The HIPPARCOS and TYCHO Catalogues. Astrometric and Photometric Star Catalogues Derived from the ESA HIPPARCOS Space Astrometry Mission
Fischer, D. A., & Marcy, G. W. 1992, ApJ, 396, 178
Folsom, C. P., Wade, G. A., & Johnson, N. M. 2013, MNRAS, 433, 3336
Girardi, L., Bressan, A., Bertelli, G., & Chiosi, C. 2000a, A&AS, 141, 371
Girardi, L., Bressan, A., Bertelli, G., & Chiosi, C. 2000b, VizieR Online Data Catalog, 414, 10371
Gray, D. F. 2005, The Observation and Analysis of Stellar Photospheres (3rd edn. Cambridge: Cambridge Univ. Press)
Hartkopf, W. I., McAlister, H. A., & Mason, B. D. 2001, AJ, 122, 3480
Hauck, B., & Mermilliod, M. 1998, A&AS, 129, 431
Høg, E., Fabricius, C., Makarov, V. V., et al. 2000, A&A, 355, L27
Horch, E. P., Falta, D., Anderson, L. M., et al. 2010, AJ, 139, 205
Horch, E. P., Gomez, S. C., Sherry, W. H., et al. 2011, AJ, 141, 45
Horch, E. P., van Altena, W. F., Cyr, Jr., W. M., et al. 2008, AJ, 136, 312
Kurucz, R. 1994, Solar Abundance Model Atmospheres for 0,1,2,4,8 km/s. Kurucz CD-ROM No. 19. (Cambridge, Mass.: Smithsonian Astrophysical Observatory)
Lang, K. R. 1992, Astrophysical Data I. Planets and Stars.

(Springer-Verlag Berlin Heidelberg New York), 33
Maíz Apellániz, J. 2007, in Astronomical Society of the Pacific Conference Series, 364, The Future of Photometric, Spectrophotometric and Polarimetric Standardization, ed. C. Sterken, 227
Malkov, O. Y., Sichevskij, S. G., & Kovaleva, D. A. 2010, MNRAS, 401, 695
Masda, S. G., Al-Wardat, M. A., Neuhäuser, R., & Al-Naimiy, H. M. 2016, RAA (Research in Astronomy and Astrophysics), 16, 112
Mason, B. D., Hartkopf, W. I., & Tokovinin, A. 2010, AJ, 140, 735
Mason, B. D., Martin, C., Hartkopf, W. I., et al. 1999, AJ, 117, 1890
Monet, D. G. 1977, ApJ, 214, L133
Pluzhnik, E. A. 2005, A&A, 431, 587
Schlegel, D. J., Finkbeiner, D. P., & Davis, M. 1998, ApJ, 500, 525
Shatskii, N. I., & Tokovinin, A. A. 1998, Astronomy Letters, 24, 673
Tokovinin, A. 1992, in Astronomical Society of the Pacific Conference Series, 32, IAU Colloq. 135: Complementary Approaches to Double and Multiple Star Research, eds. H. A. McAlister, & W. I. Hartkopf, 573
Tokovinin, A., Cantarutti, R., Tighe, R., et al. 2010a, PASP, 122, 1483
Tokovinin, A., Mason, B. D., & Hartkopf, W. I. 2010b, AJ, 139, 743
Tokovinin, A., Mason, B. D., & Hartkopf, W. I. 2014, AJ, 147, 123
Tokovinin, A., Mason, B. D., Hartkopf, W. I., Mendez, R. A., & Horch, E. P. 2015, AJ, 150, 50
Tokovinin, A., Mason, B. D., Hartkopf, W. I., Mendez, R. A., & Horch, E. P. 2016, AJ, 151, 153
van Leeuwen, F. 2007, A&A, 474, 653
Zinnecker, H., & Mathieu, R., eds. 2001, IAU Symposium, 200, The Formation of Binary Stars